Revista de acesso livre no site www.ufcg.edu.br

Revista Eletrônica de Materiais e Processos, v. 13, n. 2 (2018) 108-113
ISSN 1809-8797

REMAP

Modelling Erosion in Surfaces of a Ductile Material Impacted by Irregular Polyhedral Particles

M.A. Minguta[1], A. Marinho Junior[1]

[1] Mechanical Engineering Department – Rio de Janeiro State University – PPGEM/UERJ – 2332-7434, Rio de Janeiro,RJ

(Recebido em 06/05/2018; revisado em 08/08/2018; aceito em 14/02/2019)
(Todas as informações contidas neste artigo são de responsabilidade dos autores)

Abstract:
In simulations of surface erosion, impacting particles have been systematically modeled as spheres. The use of other particle shapes, closer to reality, was the motivation for this work. In it, a non-linear finite element analysis was carried out in order to simulate, in 3D configuration, this type of erosion in surfaces of a ductile material. Impacts were done by rigid particles with irregular polyhedral, as well as with spherical and cubic shapes. Being a case of dynamic compression in an elastoplastic target material, involving effects of strain hardening, strain-rate and temperature, a Johnson and Cook formulation was used. Images from these simulations were compared to SEM images from previous experiments with a ductile material, the Duplex Stainless Steel UNS S32205, where their surfaces were eroded by impact of alumina particles entrained in air flux. Results of simulations were compared to those of experiments, considering the morphology, dimensions of erosion craters and evidence of mass loss. In simulations, results with irregular polyhedral particles reproduce the experimental ones better than those obtained with other shapes. Despite this, it was observed that simulations with spherical particles still remain useful. Additionally, simulations with polyhedral particles suggest further studies on a possible combination of two traditional models for erosion by impacting particles in ductile materials.

Keywords: Solid Particle Erosion; Numerical Simulation; Ductile materials

1. Introdução

Degradation of engineering materials is a matter of economics. Billions of dollars are expended annually to improve design and to prevent and control the deleterious effects of this phenomenon [1,2]. Erosion of surfaces, especially in case of impact of hard particles entrained in moving fluids, is a relevant issue in design, operation and maintenance of pumps, turbines, separators, valves and tubes, as well as in structures [3-8].

In ductile metals, the erosion craters play a relevant role in elucidating the phenomenon and there is a model (‘localization’) [9, 10] based on the effects of successive impacts of single particles, on the same point of a surface. This model explains erosion in ductile materials better than others models, like the “cutting” model [7], which applies, for example, to surface ploughing in machining and to erosion by impacts with shallow angles of impingement. Both models are shown in Fig. 1, the cutting model in (A) and the localization in (B). According to the localization model, the craters initiation and evolution are shown in (B): in a first impact on the surface (a), a particle can have sufficient energy to; at least, cause a localized plastic deformation in the target material, creating a crater (b). A second impact on this crater can increase deformation on the bottom of it, strain hardening the material and creating plastically deformed borders, or “lips” (c). From the following impact on, the target material could be submitted to strain conditions leading to fracture along a heavily sheared layer at the base of the lip. The detachment of the lip characterizes the loss of mass, i.e. erosion. This is attributed to cracks in a narrow region of very large shearing, called Adiabatic Shear Band (ASB).

Successive impacts of hard particles, in surfaces of ductile materials involve effects of dynamic compression. Thus, in simulations, high strain-rate plastic deformation of ductile materials can be described by constitutive equations that link stress with strain, strain rate, and often temperature [11]. Part of the plastic work is converted into heat, and as the temperature in the material increases, the flow stress usually tends to decrease. There are many formulations relating those variables; one of them is the Johnson and Cook formulation [12].

Several works on simulation of erosion by impact of particles consider spherical rigid particles [13-19]. Finite element software is often used and, to simulate material failure, it is necessary to define a damage initiation criteria and its respective damage evolution law

.

*E-mail: maria.uerj@gmail.com (M.A. Minguta)

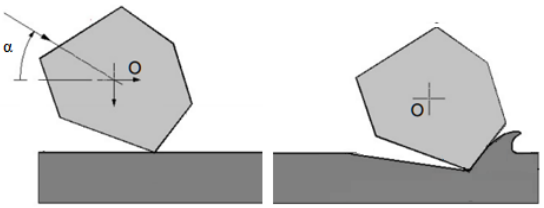

(A) Cutting model

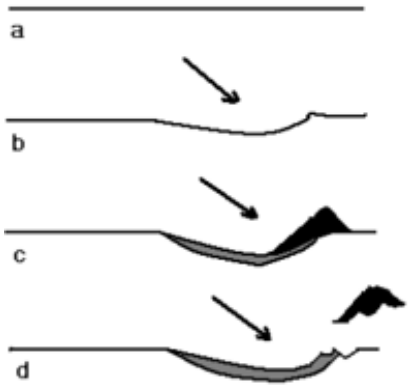

(B) Localization model

Figure 1: Erosion models. Source: Adapted from [7, 9].

The damage evolution law describes the rate of progressive degradation of the stiffness of the target material, until the corresponding damage initiation criterion had been reached, leading to material failure [20].

The present work aimed to simulate the surface erosion of a ductile material by impact of individual rigid particles, focusing in irregular polyhedral shape. Three analyses were carried out with erodent particles also modeled as spherical and cubic. The observations of erosion effects were concentrated on craters and their morphology, dimensions, lip formation, and mass loss evidences. For comparison, it was considered the results of a previous experimental work [21] [22], where surfaces of a commercial hot rolled plate of a Duplex Stainless Steel (DSS) UNS S32205 were eroded by impact of alumina particles entrained in turbulent air flux. These particles had an irregular polyhedral shape, 100 mesh (150 µm) speed of 50 m/s and were oriented 30º with the block surface. Alumina was chosen by its erosive effectiveness [23]. SEM images allowed observing, on eroded surfaces, the consequences of particle impacts in different conditions. Additionally, the applicability of models for erosion by impact of solid particles in ductile materials was discussed.

2. Materials and Methods

2.1 Modelling

The erosion process was modelled in a dynamic and adiabatic analysis, using a commercial finite element solver, the Abaqus/Explicit (version 6.13). Three analyses were performed based on an assembly containing a deformable rectangular plate 0.2 mm x 0.4 mm x 0.3 mm for the target material and rigid bodies for erodent particles. To match experimental parameters, each particle was oriented 30° with the top surface of the target, had a speed of 50 m/s, and was aligned and spaced apart, as shown in Figure 2.

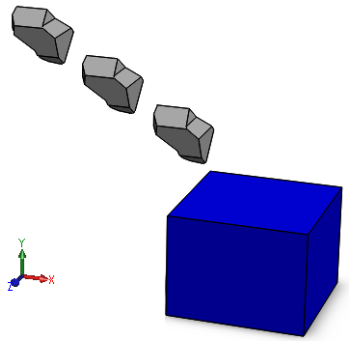

Figure 2: Assembly – polyhedral particles. Source: [Author].

In this solver, it is necessary to set some definitions as detailed next.

2.2 Geometry

The settings, in this section of the solver, are shown in Table 1.

Table 1: Settings in software geometry section.

Particle Shape/Size [mm]	Inter-Particles Spacing [mm]	Mesh Element Size
Sphere [Ø 0.150]	2 (mm)	0.004
Cube edge [0.121]	0.4 (mm)	0.002
Polyhedron [0.150]	2 (mm)	0.004

Volume and mass of each of the three types of rigid particles were the same. To simulate alumina particle, a mass of 6.9x10-6 g was associated to their centroid, as well as a density of 3,490 kg/m3. In the simulation with cubic particles, the first contact between particle and target was set to be done by the vertex of the cube, being this approach considered the worst scenario. The polyhedral particle´s shape was defined arbitrarily, as shown in Figure 4, the closer as possible of the experimental particles showed in Figure 3. In simulation, the contact was done by a small edge.

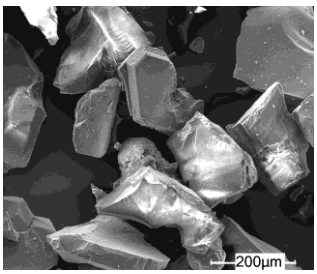

Figure 3: Geometry of alumina particles. Source: [22].

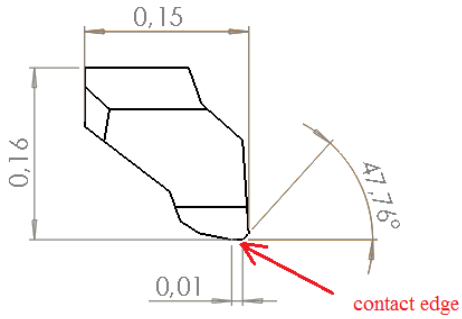

Figure 4: Arbitrarily defined polyhedral geometry. Source: [Author].

2.3 Material properties

The target material was modeled as having properties close to the DSS UNS S32205, using the Johnson and Cook formulation [24]. In this model the flow stress (σ) is expressed as a function of the strain (first term), the strain-hardening (second term) and the temperature (third term), as shown in the equation (1).

$$\sigma = [A + B\varepsilon^{n}]\left[1 + C\ln\left(\frac{\dot{\varepsilon}_{eq}}{\dot{\varepsilon}_0}\right)\right]\left[1 - \left(\frac{T - T_r}{T_m - T_r}\right)^{m}\right] \quad (1)$$

where, ε is the strain, A is the true yield stress, B is the stress at $\varepsilon = 1.0$, n is the strain-hardening coefficient, $\dot{\varepsilon}_{eq}$ is the strain rate, $\dot{\varepsilon}_0$ is the reference strain rate (usually 1.0), T is the current temperature, T_r is the room temperature, T_m is the melting temperature and m is the temperature index. Those coefficients can be obtained by specifics tests [24].

Heat generated by plastic deformation is considered in the analysis and the inelastic heat fraction (β) was set as 0.9 [11]. It is also important to define the material density (ρ) and specific heat (C_p). The temperature variation is then calculated by the equation (1) combined with the Johnson and Cook formulation.

$$\Delta T = \frac{\beta}{\rho C_p}$$

The mechanical and others properties of this material are presented in Table 2.

Table 2: Properties of target material [25].

Yield Stress 0,2%	Ultimate Tensile Stress	Elongation in 50 mm	Density	Elasticity Module	Poisson Coefficient	Hardness HRC	β	Specific Heat [J/Kg.K]
586 MPa	784 MPa	34%	7,839 kg/m^3	200 GPa	0.3	19	0.9	477

The constants of the Johnson and Cook formulation, adapted to represent the DSS UNS S32205, are in Table 3.

Table 3: Parameters of Johnson e Cook plasticity model [24] [25] [27].

A	B	n	T_m	T_r	m	C	$\dot{\varepsilon}_0$
587.2 MPa	754 MPa	0.471	1793 K	298 K	1.03	0.014	1.0 s^{-1}

2.4 Damage model

Johnson and Cook damage criteria [24] considers the damage initiate when the plastic strain is equal to the obtained by the equation (3), which depends on the strain, the strain-rate and the effect of the temperature.

$$\bar{\varepsilon}_0^{pl} = [d_1 + d_2\exp(d_3\eta)]\left[1 + d_4\ln\left(\frac{\dot{\varepsilon}^{pl}}{\dot{\varepsilon}_0}\right)\right]\left[1 + d_5\frac{T - T_r}{T_m - T_r}\right] \quad (3)$$

where, $\bar{\varepsilon}_0^{pl}$ is the plastic strain at the damage initiation, $d_1 - d_5$ are the material damage constants.

Two damage criteria were considered in the analysis, with their respective laws of evolution: the Johnson and Cook damage criterion and the shear criterion. The damage parameters are shown in Tables 5 and 6. Values for Table 5 were taken from [26] as they were not found in the literature for the DSS UNS S32205.

The damage evolution law [20], in terms of displacement, was represented by a factor 0.003 for both criteria. The factor value was fitted in an analysis using spherical particles in order that elements deletion only occurs after three particles impacts. Then, used for all analysis.

Table 5: Parameters of Johnson e Cook damage model [26].

D_1	D_2	D_3	D_4	D_3
0.05	3.44	2.12	0.002	0.61

Table 6: Parameters of shear damage model [25].

ε_{pl}	θ_s	$\dot{\varepsilon}_{pl}$
0.34	0.6	1.0 x 10-4 s^{-1}

2.5 Contact

A "surface to surface" contact type was defined between the erodent particles and the target surface. It was chosen the external surface of the rigid particles (sphere, cube and polyhedron, in their respective analysis) as master surface and a node of the target as slave surface. The properties of the contact were "normal behavior" and friction coefficient was 0.2 [17].

2.6 Mesh

Eight–nodded brick elements (C3D8R) with reduced integration and maximum degradation were used to mesh the target, while four-point tetrahedral elements (R3D4) were used for the rigid particles. For both geometries, mesh size of 0.004. An analysis of mesh sensitivity was carried out.

2.7 Boundary conditions

For the rigid bodies (erodent particles), rotation and lateral displacement were restrained. The bottom of the target plate was fixed in all simulations.

3. Results and Discussion

Comparing the images from spherical particles analysis, Fig. 5, with the (c) stage of "localization" model [9] described in Fig. 1 (B), it could be noted that they satisfactorily represent the morphological aspects (evidences of crater formation and plastic deformation) of craters and their evolution under erosion by successive impacts of hard particles in ductile materials. These results are in accordance with [13-19].

In the images in Figure 6 it was observed that, in the case of craters created exclusively by plastic deformation, the simulation with spheres reproduces the cross-section profile of the experimental craters.

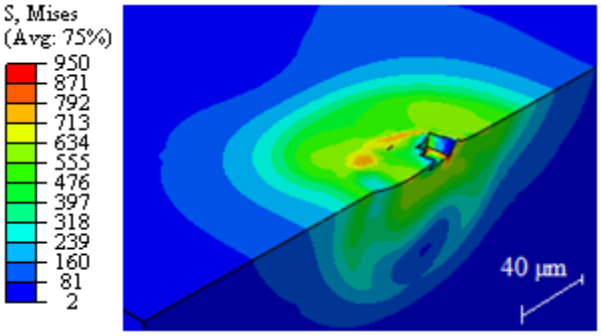

Figure 5: craters morphology after 3 impacts of spherical particles.

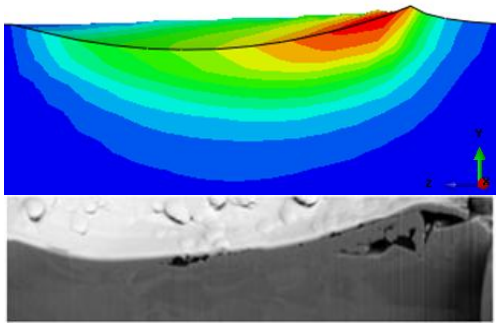

Figure 6: Cross-section profiles comparison: simulation x experiment [28].

However, the analysis with spherical particles seems not reproduce experimental craters (irregular shape) that include plugging effect. Then, another simulation with cubic particles was carried out.

The analysis with cubic particles presented results that, when compared with those obtained in experiments, meant a better representation of the effects of erosion by irregular shaped particles impacts. This can be seen in Figure 7 where, in addition to the apparently deeper craters, due to vertex-type contact, it is possible to see a more effective representation of lip formation, not only on borders, but also in the opposite side of the impact orientation. Additionally, it can be seeing the occurrence of micro cutting (like in machining). Besides, it was observed deletion of elements just after the first impact. These facts were not verified in the simulation with spherical particles and they are not expected under the localization model.

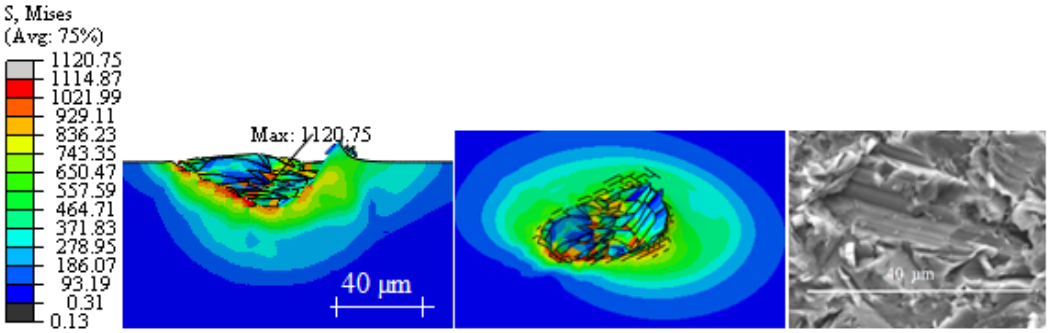

Figure 7: craters morphology after impact of particles. SEM - 5 s erosion effect [21].

Simulation with polyhedral particles provided an even better representation of the effects of erosion by irregular shaped particles impacts. It can be observed in Figure 8 that the shape of the simulated craters approaches the experimental ones in view of their elliptical shape and borders formation. These craters were shallower than in the case of cubic particle simulation.

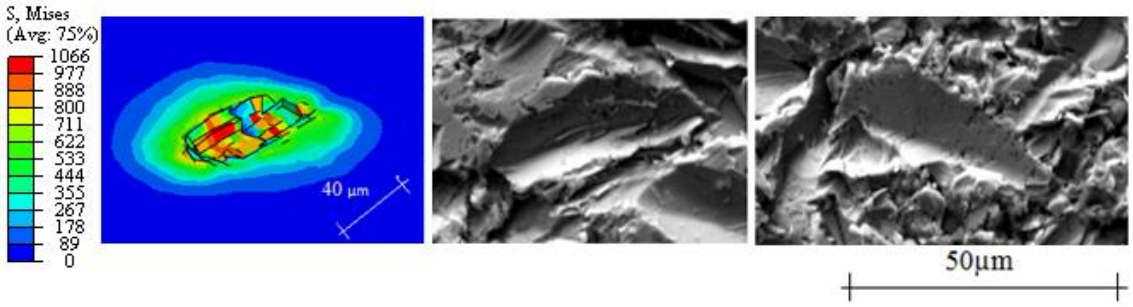

Figure 8: Morphological comparison: simulation [22] x experiment [21] [28].

Independently of the arbitrarily irregular polyhedral shape adopted for the simulated particles, the very effect of them on target surface was due to the contact of a small edge, instead of a vertex in case of cubic particles.

It must also be pointed out that, in the experiments, there was a turbulent flux of polyhedral particles. So, despite a mean angle of 30° and a mean speed of 50 m/s, the impacts were not of the same type, neither in orientation nor in kinetic energy. In experiments, evidences of cutting can be found not only in scratches but also inside plastically deformed craters.

Some measurements were made in images of craters from simulations, after three impacts, as can be seeing in Table 7. For comparison, it was included in such table the values obtained from SEM images of some experimental results.

The geometric similarity between simulated and experimental craters was roughly estimated on the basis of their length/wide ratios, assumed to be an index of ovalization.

Table 7: Craters dimensions.

Shape	**Dimension (µm)**	
	Length / Wide	Depth
	Simulation	
Spherical	56/28 = 2.0	4
Cubic	55/36 = 1.7	14
Polyhedral	60/35 = 1.7	8
	Experimental	
Polyhedral	45/25 = 1.8	7

In such aspect, craters in all cases present the same order of magnitude although, as expected, simulated craters with cubic and polyhedral particles were closer to experimental craters. In the case of the depth of craters, it became evident that simulation with spherical particles hardly reproduces the depths verified in experiments. The same applies to cubic particles, since vertex-type impacts adopted in simulations are relatively rare in reality, leading to deeper crater. Otherwise, depth values from simulations with polyhedral irregular particles matched the experimental ones. This could be attributed not only to the fact that the polyhedral particle in simulation was geometrically closer to the particles used in the experiments, but to the edge-type contact.

Concerning erosion models, it seems that the morphological aspects of the craters observed in the images suggest that the localization model is not enough to explain the morphology of some craters. In them, especially in case of experiments and in simulations with cubic and irregular polyhedral particles, it was possible to see cutting effects.

Conclusions

Simulations of erosion by impacts of solid particles were made in a ductile material. The simulated particles were of different shapes: spherical, cubic and irregular polyhedral. Based on the results of simulations and of the experimental results with a DSS UNS S32205, it was possible to conclude:

In simulations, the use of polyhedral particles, when compared to spherical and cubic ones, better reproduced the experimental results, regarding the morphology, geometry and dimensions of craters. Additionally, with this type of simulated particles, it was possible to detect evidences of cutting in plastically deformed craters, in a way more realistic than with cubic particles, where this effect was exaggerated.

The spherical particles, commonly used in simulations, appear to be still interesting, but they only represent the general morphology and the order of magnitude of experimental craters. A relevant discrepancy was observed in the depth of simulated craters, compared to experimental, and an apparent inability to show eventual cutting effects.

Considering that the localization model for erosion of ductile materials was established with spherical particles, the results of the simulations pointed out to further studies toward a possible association of the localization model with the cutting model.

Acknowledgment

The authors are grateful to TESCAN for the use of an image and to FAPERJ, for a MS fellowship to Maria Augusta Minguta.

Referências

[1] E Stachoviak, G. H., Batchelor. A. W., "Engineering Tribology", Elsevier. Amsterdam, 2nd Ed. Vol. 1, pp 1-9, 1993.

[2] Nace, International Corrosion Cost and Preventive Strategies in the United States, NTIS, 2002. http://isddc.dot.gov/OLPFiles/FHWA/011536.pdf Access in: 09/11/2015.

[3] Batchelor, A. W, Chandrasekaran, M., "Introduction: Materials degradation and its control by surface engineering", 3rd Ed, Imperial College Press London, vol. 1, pp 1-9, 2011.

[4] Bhushan, B. "Tribology: Friction, Wear and Lubrication". In: The Engineering Handbook, Ed. Richard C. Dorf, CRC Press LLC Boca Raton, 2000.

[5] Hutchings, I. M. "Friction and Wear of Engineering Materials". In: Tribology: Ed. Butterworth-Heinemann, p. 273, 1992.

[6] Bitter, J. "A study of erosion phenomena", part 1&2, Wear, vol. 6, pp 161-190, 1963.

[7] Finnie, I. "Some Observations on the Erosion of Ductile Metals". Wear, vol. 19, pp 81-90, 1972.

[8] Winter, R. E. and Hutchings, I. M. "Solid particle erosion studies using single angular particles". Wear, vol. 29, pp 181-194, 1974.

[9] Shewmon, P., Sundararajan, G. "The Erosion of Metals", Ann. Rev. Mater. Sci., vol. 13, pp 301-18, 1983.

[10] Sandararajan, G.,Roy, M. "Solid particle erosion behavior of metallic materials at room and elevated temperatures". Tribology International, vol. 30, pp 339-359, 1997.

[11] Meyers, M. A. "Dynamic Behavior of Materials". University of California, San Diego. Ed. Wiley. 1994.

[12] Wright, T. W. "The physics and mathematics of adiabatic shear bands". Army Research Laboratory. Cambridge University Press. Chap 1, pp 1-34, 2002.

[13] Elalem, K. T. "Development of a micro-scale dynamic model for wear simulation". 159 pages. Thesis (PhD – Chemical and Materials Engineering) – University of Alberta, United States, 2000.

[14] Shimizu, K.; Noguchi, T; Seitoh, H; Okadab, M. Matsubara, Y.; FEM "Analysis of erosive wear". Wear (250) pp 779-784, 2001.

[15] Aquaro, D; Fontani, E. "Erosion of ductile and Brittle Materials". Meccanica, vol. 36, pp 651-661, 2001.

[16] Chen, Q.; Li, D.Y. "Computer Simulation of Solid Particle Erosion wear". Wear. Vol. 254, pp 203-210, 2003.

[17] Eltobgy, M. S., E. NG, Elbestawi, M. A. "Finite element modeling of erosive wear". International Journal of Machine Tools & Manufacture. Vol. 45, pp 1337-1346, 2005.

[18] Aquaro, D. "Erosion due to the impact of solid particles of materials resistant at high temperature". Meccanica. Vol. 41, pp 539-551, 2006.

[19] Aquaro, D. "Erosion rate of stainless steel due to the impact of solid particles". AITC-AIT International Conference on Tribology, Parma, Italy, 2006.

[20] Abaqus. "Analysis User´s Guide". Vol. 1, 2, 3, 4 e 5. 4979 páginas. Dassault Systèmes. 2014.

[21] Santos, A. C. "Morfologia e Topografia de Superfícies de Aço Inoxidável Duplex UNS S32205, submetidos à Erosão por Impactos de Partículas de Alumina em Fluxo de Ar". 103 páginas. Dissertação (Mestrado – Engenharia) - Universidade do Estado do Rio de Janeiro, Rio de Janeiro, 2014.

[22] Minguta, M. A. "Erosão por impacto de partículas – Caracterização e simulação da ocorrência de Cisalhamento Adiabático (ASB) em aço inoxidável duplex UNS S32205". 117 páginas. Dissertação (Mestrado – Engenharia) - Universidade do Estado do Rio de Janeiro, Rio de Janeiro, 2017.

[23] Desale, G. R., Ghandi, B. K., Jain, S. C. "Effect of erodent properties on erosion wear of ductile type materials". Wear, vol. 261, pp 914–921, 2006.

[24] Johnson, G. R., Cook, W. H. "A constitutive model and data for metals subjected to large strains, high strain rates and high temperatures". Proc. 7th Int. Symp. on BuNistics, pp. 541-547. The Netherlands. April, 1983.

[25] Sandmeyer Steel Company. "Certified Material Test Report, SSC Order 74847, Costumer Order 14248", 07/26/2013.

[26] Johnson, G. R., Cook, W.H. – "Fracture characteristics of three metals subjected to various strain rates, temperatures and pressures"– Engineering Fracture Mechanics, vol 21, No. 1, pp 31-48, 1985.

[27] Tavares, S.S.M., Pardal, J. M., Abreu, H. F. G., Nunes, C. S., Silva, M. R. "Tensile Properties of Duplex UNS S32205 and Lean Duplex UNS S32304 Steels and the Influence of Short Duration 475 °C Aging". Materials Research, vol. 15(6), pp 859-864, 2012.

[28] Tescan, Sample Analysis Report, Reference Number 16-179, 2016.